Amino Acids and Proteins at ZnO-water Interfaces in Molecular Dynamics Simulations: Electronic Supplementary Information

Grzegorz Nawrocki and Marek Cieplak
Institute of Physics, Polish Academy of Sciences, Al. Lotników 32/46, 02-668 Warsaw, Poland

April 5, 2013

Electrostatic potential near ZnO surfaces

The simulations described in the paper can be performed in two equivalent ways. One is to introduce a cutoff in all Coulombic interactions and then using the periodic boundary conditions with the particle mesh Ewald summation [1]. The other is to treat the static electric field of the semi-infinite solid as external to the molecular interactions and then use the Ewald summation only for the "internal" interactions. Here, we discuss the properties of the electrostatic potential, ϕ, generated by ZnO that could be used in the second way. The potential is non-uniform very near the surface but it becomes practically uniform at a sufficiently large elevation. It is interesting to find out how does the transition between the two regimes take places.

We construct the surfaces by making planar cuts in the bulk solid generated by translating the unit cell. The ϕ potential is determined at sites on a grid spaced by d =0.01 nm extending 5 nm above and 0.5 nm below the surface. The solid is represented by a slab of layers of the unit cells. For every grid point, we consider a vertical cylinder with radius R and the axis going through the grid point. The cylinder contains an integer number of the unit cells so its sides are rough. The atoms within this cylinder contribute to the Coulombic sum $C(x,y,z) = f\sum_i \frac{q_i}{r_i}$, where r_i is the distance from the grid site to the i'th atom, q_i is its charge and f=138.935485 kJ mol^{-1} nm e^{-2} is the conversion factor. The effective charges are -1.026e and 1.026e for the O and Zn atoms respectively, as obtained through the Mulliken analysis [2]. The sums are calculated for a set of values of R up to 500 nm and then extrapolated to an infinite R by fitting to $\frac{R_0}{R} + \phi(x,y,z)$ (R_0 is another fitting constant) – see Figure 1 for z=0.2 nm and x=y=0.0, i.e. at the O atom. The values of $\phi(x,y,z)$ are stored. The electric field is obtained through discretized differentiation. For instance, its z-component is given by $E_z(xyz) = [\phi(x,y,(z-d)) - \phi(x,y,(z+d))/2d$. The values of ϕ and $\vec{E}$ away from the grid points can be obtained through interpolation involving the 8 nearest grid nodes.

The electrostatic potential due to the surface has a lateral structure that depends on z. Above z ≈0.4 nm the electric field becomes uniform and close to zero for each surface. Modulations in the density of water persist above 0.4 nm as they are induced by the field at lower elevations. It is sufficient to take two layers of cells in the slab – the slab is about 0.5 nm wide. Combining, say, 10 slabs one atop another either does not change the ϕ or, in the case of the polar surfaces, merely adds a constant.

An alternative way to determine ϕ is by considering larger and larger spheres of radius R (up to 1 μm) that are cut out in the bulk solid and are centered at the grid point. The spheres contain same numbers of the Zn and O atoms, but fractional numbers of unit cells. Therefore, the nature of the net polarization keeps oscillating which results in the oscillatory nature of the potential. Extrapolation to an infinite sphere is, however, consistent with the slab results (see Figure 1).

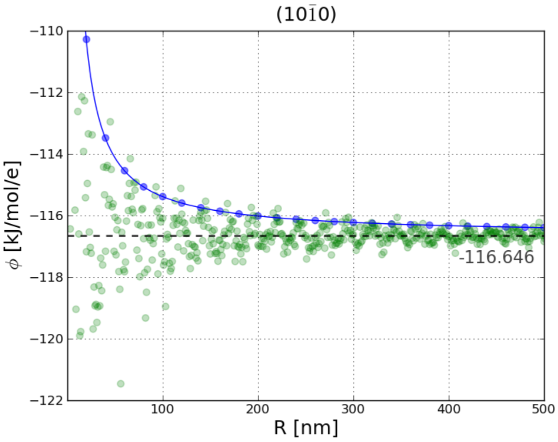

Figure 1: $\phi(R)$ for x=0.0, y=0.0 and z=0.2 position above the (10$\bar{1}$0)surface of ZnO. The dots represent the data obtained: the blue circles are for the cylindrical cutouts of radius R and green for the spherical cutouts corresponding to radius R. The blue solid line represents a fit to the cylindrical data points whereas the dashed line represents the asymptotic potential obtained for the spherical cutouts.

Figure 2 shows ϕ in the xy plane at z=0.2 nm above the (10$\bar{1}$0) surface of ZnO. Figure 3 shows ϕ as a function of z for selected locations (1 through 5) that are indicated in Figure 1. For instance, 1 is at the origin, i.e. above the O atom. 2 is above the Zn atom. 3 and 4 are above O and Zn atoms as for sites 1 and 2, but these atoms are located deeper – under the top plane of the surface. 5 is in the middle. Figure 4 shows the corresponding values of the z-component of the electric field.

The next three figures, 5, 6 and 7, are similar but they refer to surface $11\bar{2}0$. Figures 8, 9, and 10 refer to the polar surface (0001-O) and figures 11, 12, and 13 to the polar surface ($000\bar{1}$-Zn).

References

[1] U. Essmann, L. Perera, M. L. Berkowitz, T. Darden, H. Lee and L. G. Pedersen, *J. Chem. Phys.*, 1995, **103**, 8577-8592.

[2] D. Raymand, A. C. T. van Duin, M. Baudin and K. Hermannson, *Surf. Sci.*, 2008, **602**, 1020-1031.

[3] M. Hoefling, F. Iori, S. Corni and K. E. Gottschalk, *Langmuir*, 2010, **26**, 8347-8351.

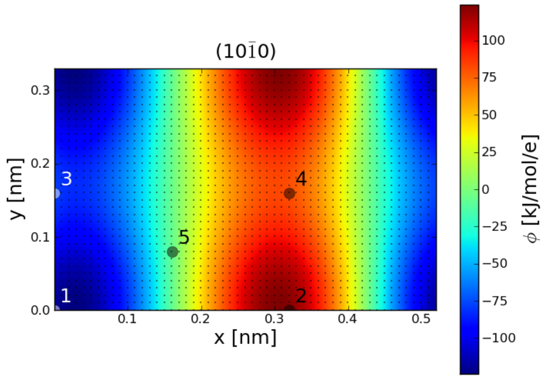

Figure 2: $\phi(xy)$ for z=0.2 nm above the (10$\bar{1}$0) surface.

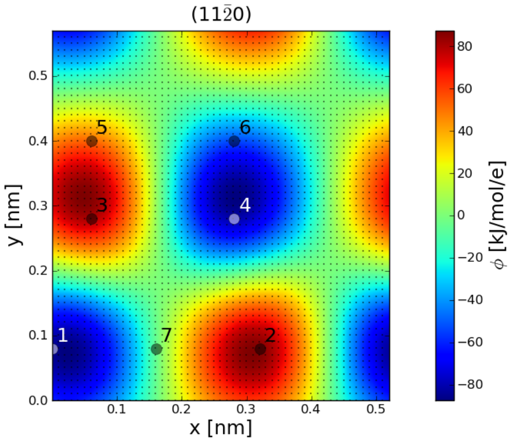

Figure 5: $\phi(xy)$ for z=0.2 nm above the (11$\bar{2}$0) surface.

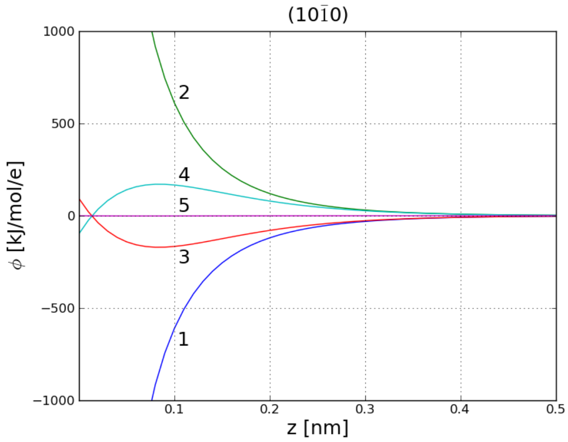

Figure 3: $\phi(z)$ for selected xy positions above the (10$\bar{1}$0) surface as indicated in Figure 2.

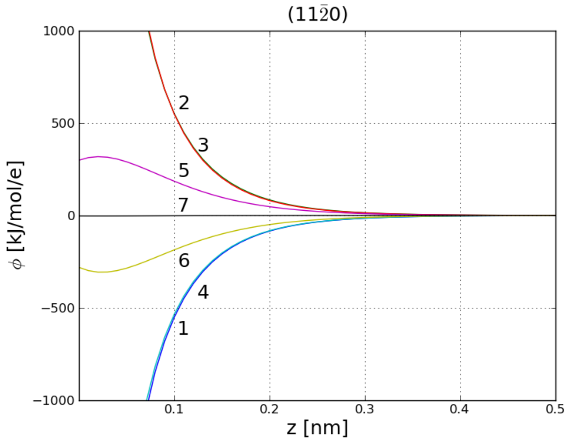

Figure 6: $\phi(z)$ for selected xy positions above the (11$\bar{2}$0) surface as indicated in Figure 5.

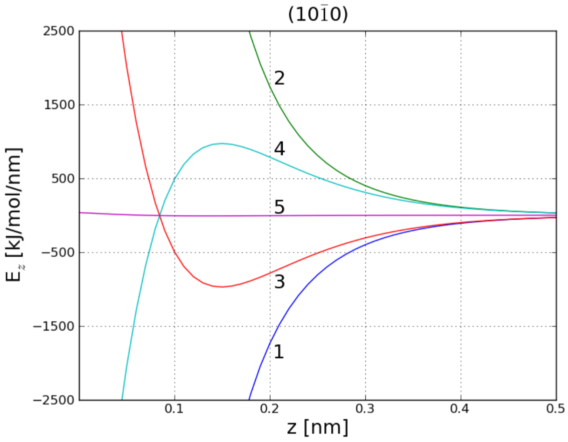

Figure 4: E$_z$ for selected xy positions above the (10$\bar{1}$0) surface, as indicated in Figure 2.

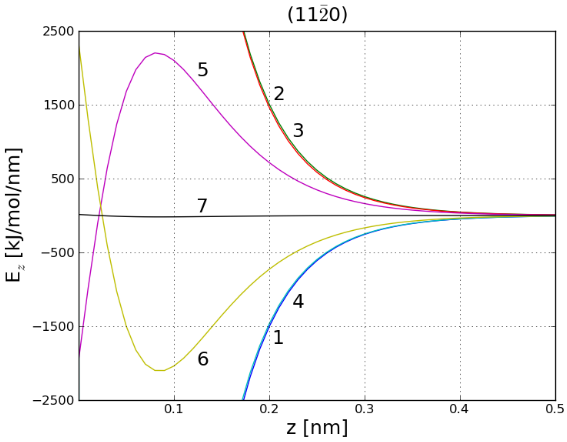

Figure 7: E$_z$ for selected xy positions above the (11$\bar{2}$0) surface, as indicated in Figure 5.

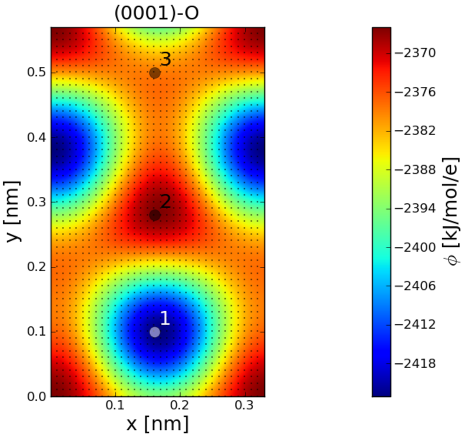

Figure 8: $\phi(xy)$ for z=0.2 nm above the (0001)-O surface.

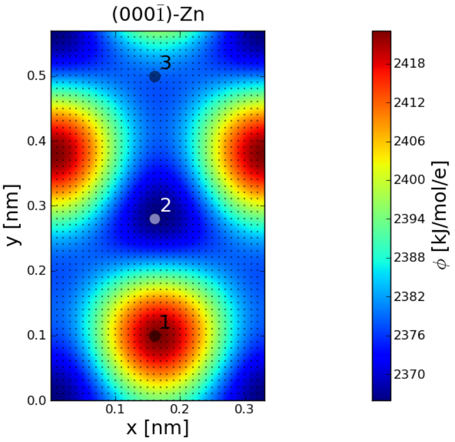

Figure 11: $\phi(xy)$ for z=0.2 nm above the (000$\bar{1}$)-Zn surface.

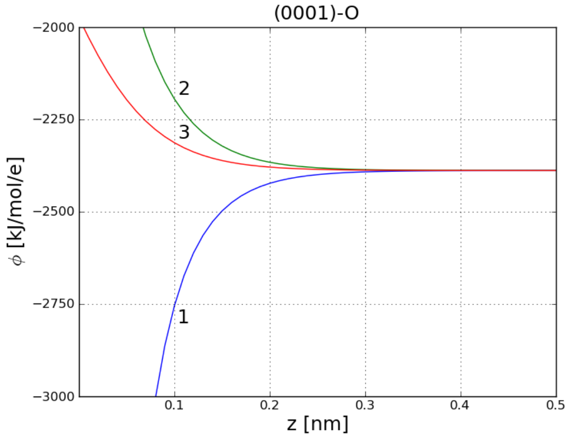

Figure 9: $\phi(z)$ for selected xy positions above the (0001)-O surface as indicated in Figure 8.

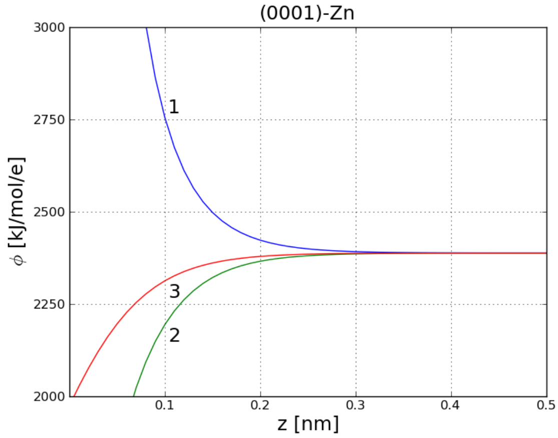

Figure 12: $\phi(z)$ for selected xy positions above the (000$\bar{1}$)-Zn surface as indicated in Figure 11.

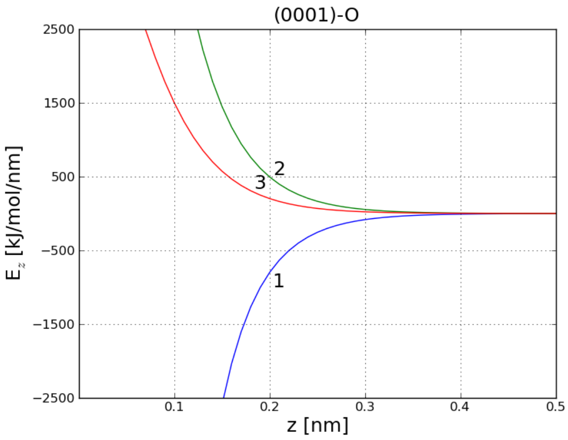

Figure 10: E_z for selected xy positions above the (0001)-O surface, as indicated in Figure 8.

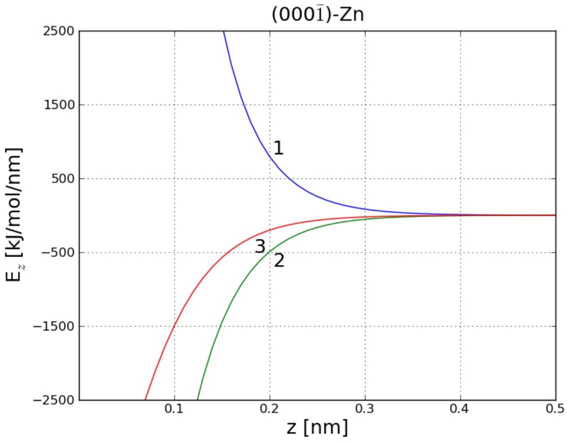

Figure 13: E_z for selected xy positions above the (000$\bar{1}$)-Zn surface, as indicated in Figure 11.

Structure of water at the solid-water interface

Figure 14 shows snapshots of the solid-water interface that illustrate the architecture of the solid and the nature of layering of water molecules for the four surfaces and at various projections. Figure 15 shows the time averaged profile of the number density of water molecules near ZnO(10$\bar{1}$0), as taken from Figure 3 in the main paper, and compares it to the profile near Au(111). The profiles are normalized so that the bulk value corresponds to 1.

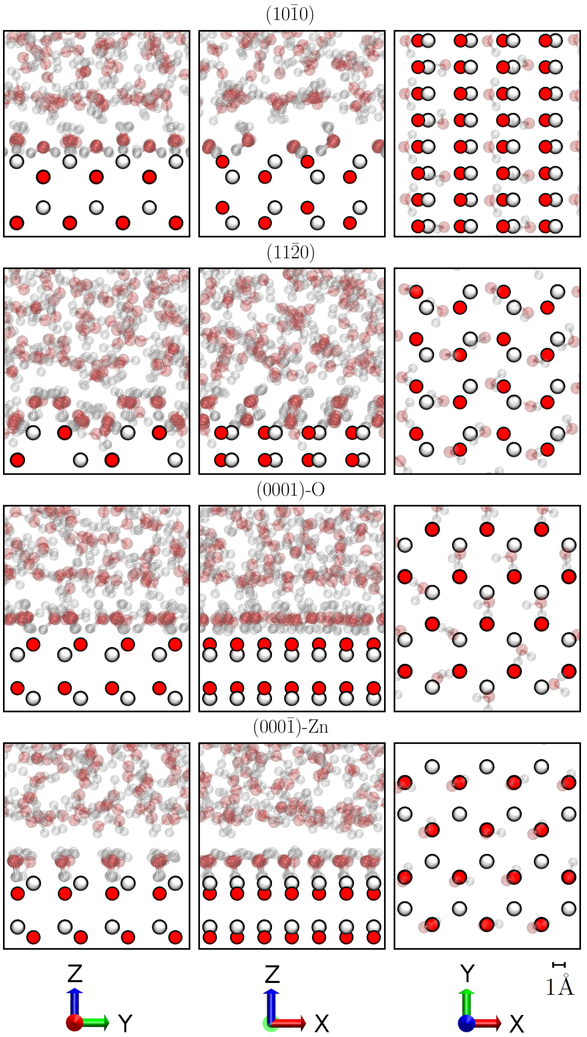

Figure 14: Snapshots of the solid-water interface for the four surfaces and at various projections. For instance, the panels on the right show the top views. The larger and stronger symbols show the solid atoms: the O atoms are in red and the Zn atoms in white. The fainter symbols correspond to the molecules of water (in the panels on the right – from the first layer). The red color is again for O and the gray symbols for the H atoms. Notice, that the H atoms in the first layer tend to face the underlying surface but in a manner that depend on the surface.

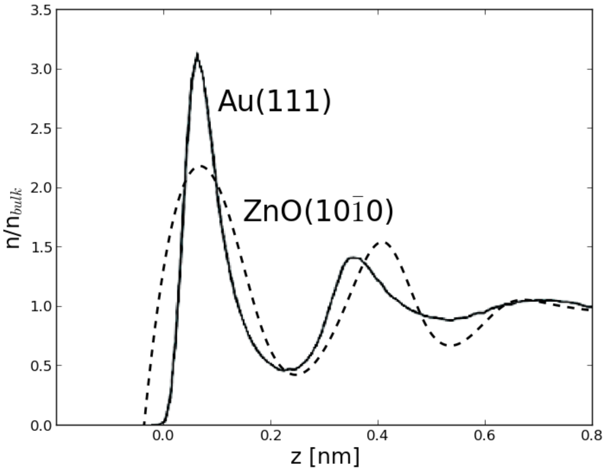

Figure 15: The solid line shows the density profile of water near Au(111) as obtained in ref. [3]. The density is normalized to its bulk value. The dashed line is the normalized profile obtained here for water molecules near the 10$\bar{1}$0 surface of ZnO. The location of the first maximum corresponding to the situation with Au(111) is adjusted to coincide with the first maximum for the ZnO problem.

The umbrella sampling method

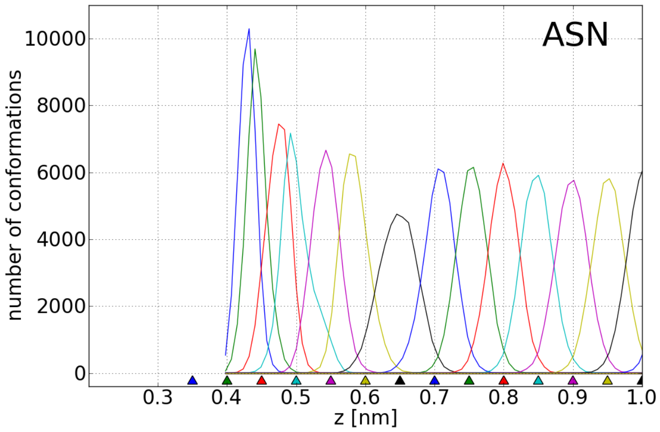

Figure 16: Histogram of the number of conformations of asparagine above the $10\bar{1}0$ surface of ZnO in water as obtained through the umbrella sampling method. The different colors correspond to various simulation windows. In each simulation, the AA is restrained by the umbrella biasing potential to different selected values of z that are marked as triangles n a color corresponding to the simulation window. For instance, the maximum of the distribution for z=0.7 nm is close to the set value, indicating a weak impact of the surface. Between 0.5 and 0.6 nm, the maxima are shifted toward the surface due to the attraction. However, below 0.5 nm, the maxima are shifted away from the surface due to the impact of the layers of water. Generally, a large shift away from the set value comes with a narrower and taller distribution. A wide distribution, as for z=0.65 nm, suggests that the AA is attracted by the surface weakly.

Summary of the results on the binding parameters

Table 1 provides an expanded version of Table 1 in the main text. In addition to items listed there it also gives values of the parameter σ for individual amino acids.

ZnO	$(10\bar{1}0)^v$		$(10\bar{1}0)$		$(11\bar{2}0)$		(0001)-O		$(000\bar{1})$-Zn	
	σ	ϵ	σ	ϵ	σ	ϵ	σ	ϵ	σ	ϵ
ASP	0.29	192.14	0.55	0.72	–	–	0.56	1.10	0.44	3.91
GLU	0.28	197.33	–	–	0.91	0.42	0.61	1.03	0.52	2.56
CYS	0.28	167.27	0.51	1.04	0.88	0.59	–	–	0.56	3.07
ASN	0.23	170.38	0.54	4.17	0.59	2.31	0.87	0.27	0.58	4.12
PHE	0.29	110.16	–	–	0.92	0.27	–	–	0.55	1.99
THR	0.31	136.39	–	–	–	–	–	–	0.58	0.51
TYR	0.29	128.26	0.90	0.17	0.63	2.00	–	–	0.54	7.01
GLN	0.27	160.66	–	–	0.63	1.01	0.95	0.48	–	–
SER	0.28	140.36	0.49	0.63	0.53	1.68	0.87	0.48	0.55	0.97
MET	0.26	123.53	–	–	0.55	2.19	0.89	0.25	0.54	0.77
TRP	0.33	165.73	0.63	3.08	0.61	0.17	–	–	0.53	4.78
VAL	0.27	135.23	1.01	0.16	0.56	1.02	0.91	0.31	0.65	1.39
LEU	0.29	142.16	0.86	0.19	–	–	–	–	0.64	1.28
ILE	0.31	126.54	–	–	–	–	–	–	0.61	2.80
GLY	0.31	116.24	0.47	2.57	0.53	0.29	–	–	0.50	2.08
ALA	0.27	110.98	–	–	0.54	1.06	0.99	0.25	0.54	2.91
PRO	0.31	121.15	0.88	0.70	0.63	0.66	1.00	0.64	0.57	2.72
HIE	0.27	194.74	–	–	–	–	–	–	0.56	0.52
HID	0.23	202.98	0.51	0.74	0.55	1.56	–	–	0.56	3.19
HIP	0.27	181.40	0.50	4.47	0.58	2.28	–	–	0.89	1.34
LYS	0.27	169.68	–	–	–	–	0.74	1.78	0.56	0.74
ARG	0.26	126.46	–	–	0.64	2.70	–	–	0.51	4.14

Table 1: Values of the binding energy ϵ [kJ mol^{-1}] and the bond length σ [nm] for the four ZnO surfaces. σ is measured between the center of mass of an AA and the surface. The symbol – signifies non-binding situations. The superscript v denotes results obtained in vacuum.

Potential of the mean force at the $(10\bar{1}0)$ ZnO interface in vacuum

Here, we provide plots of the PMF obtained by the umbrella sampling simulations for AAs above the $(10\bar{1}0)$ in vacuum – Figures 17 through 26. The binding energy varies across the AAs between 100 and 200 kJ/mol (Table I in the main text and Table 1 here). The average bond length is about 0.28 nm.

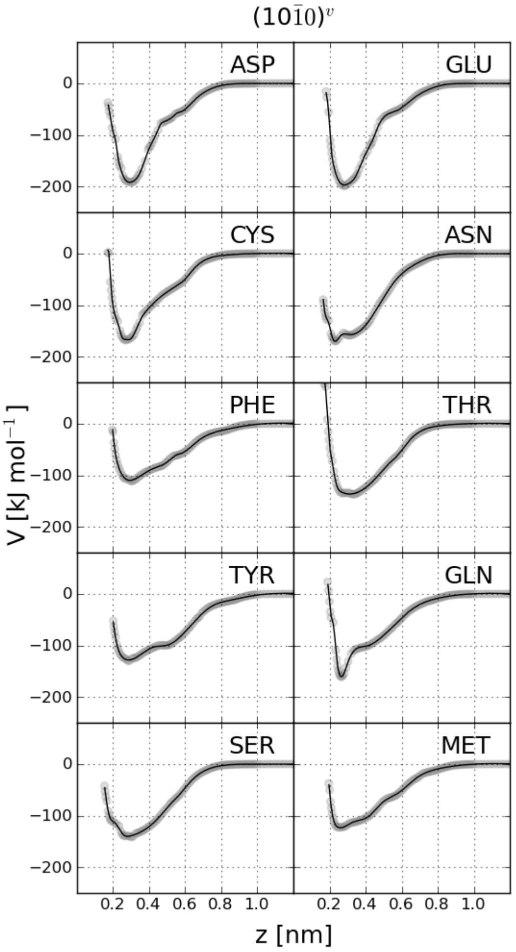

Figure 17: $V(z)$ for the AAs in vacuum.

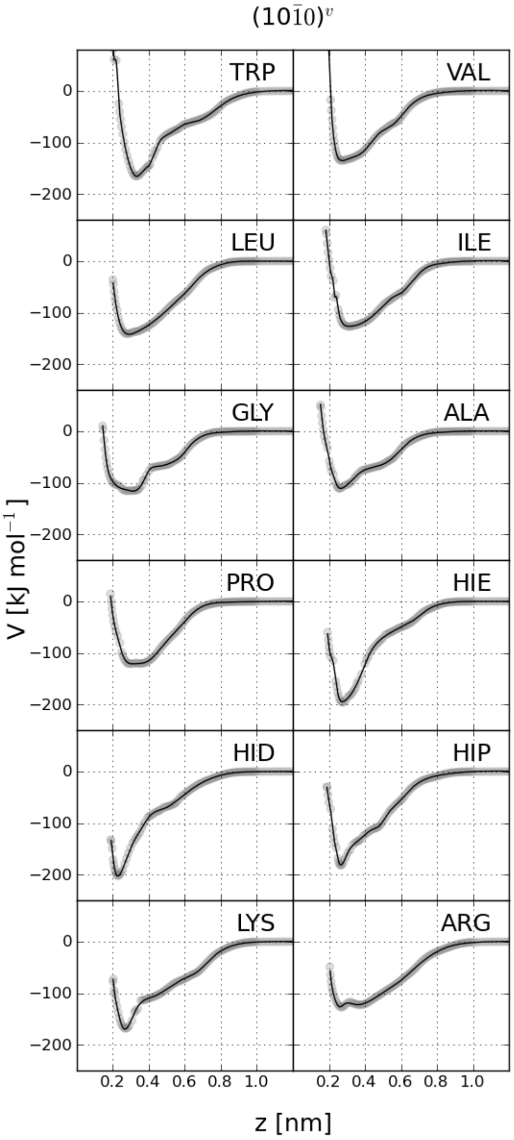

Figure 18: $V(z)$ for the AAs in vacuum – continued.

Potential of the mean force at the ZnO interfaces in water

Here, we provide plots of the PMF obtained by the umbrella sampling simulations for AAs in water – Figures 19, and 20. The binding energies are listed in Table I in the main text and Table 1 here.

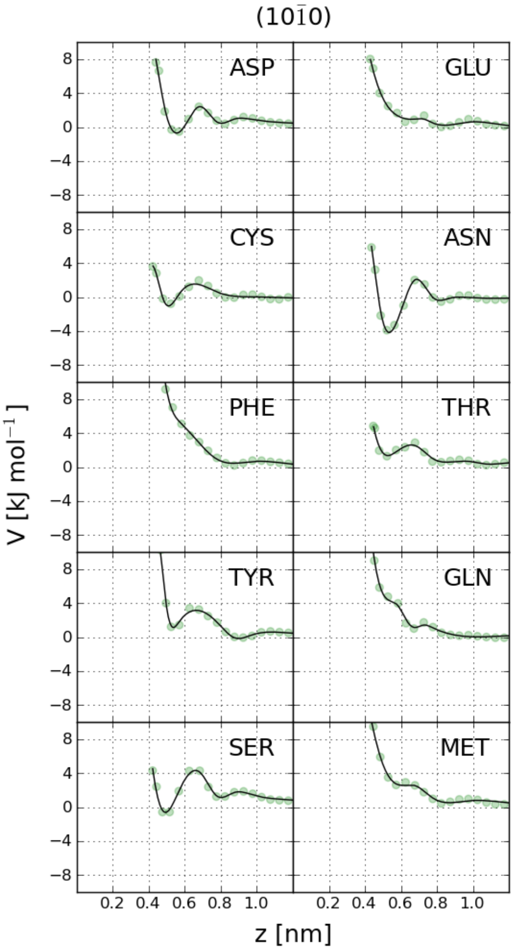

Figure 19: $V(z)$ for AAs above the (10$\bar{1}$0) surface in water.

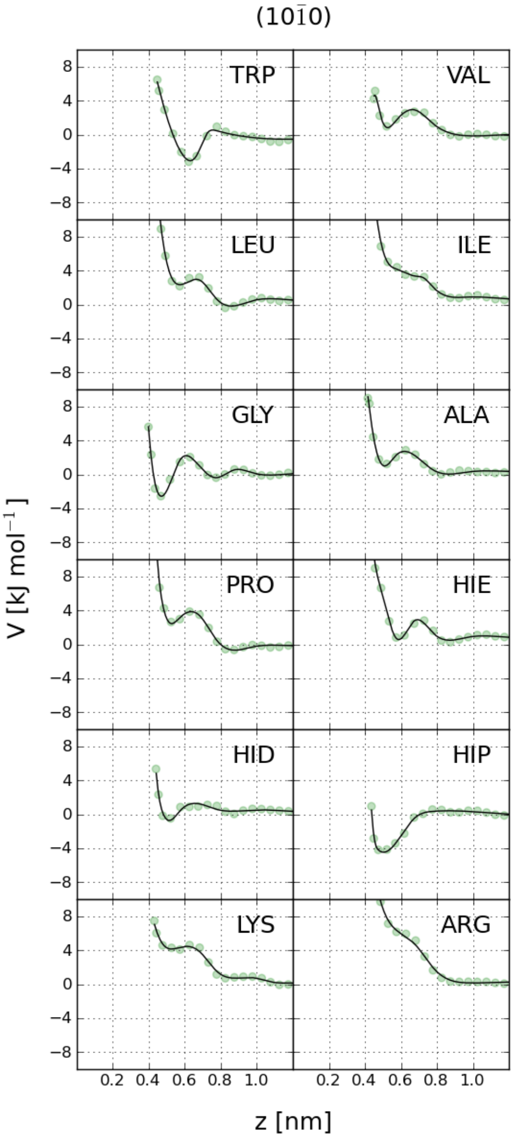

Figure 20: $V(z)$ for AAs above the (10$\bar{1}$0) surface in water – continued.

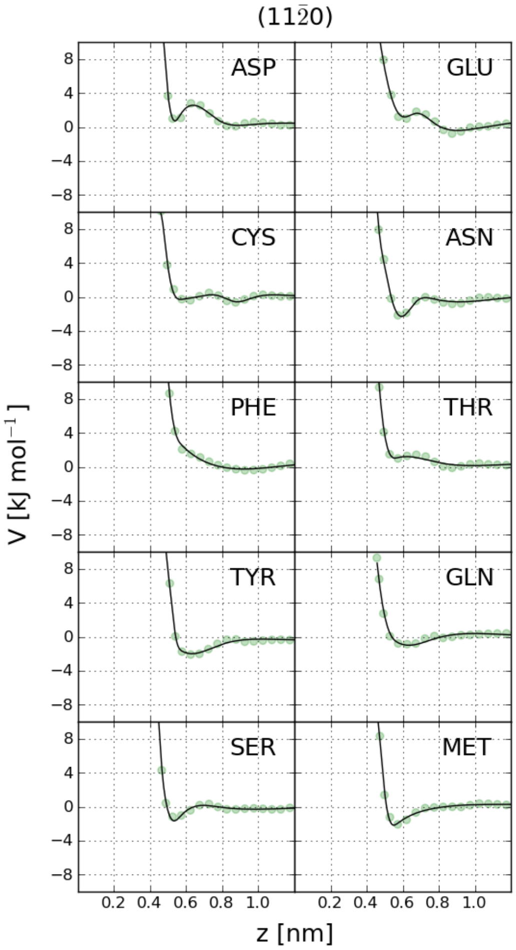

Figure 21: $V(z)$ for AAs above the (11$\bar{2}$0) surface in water.

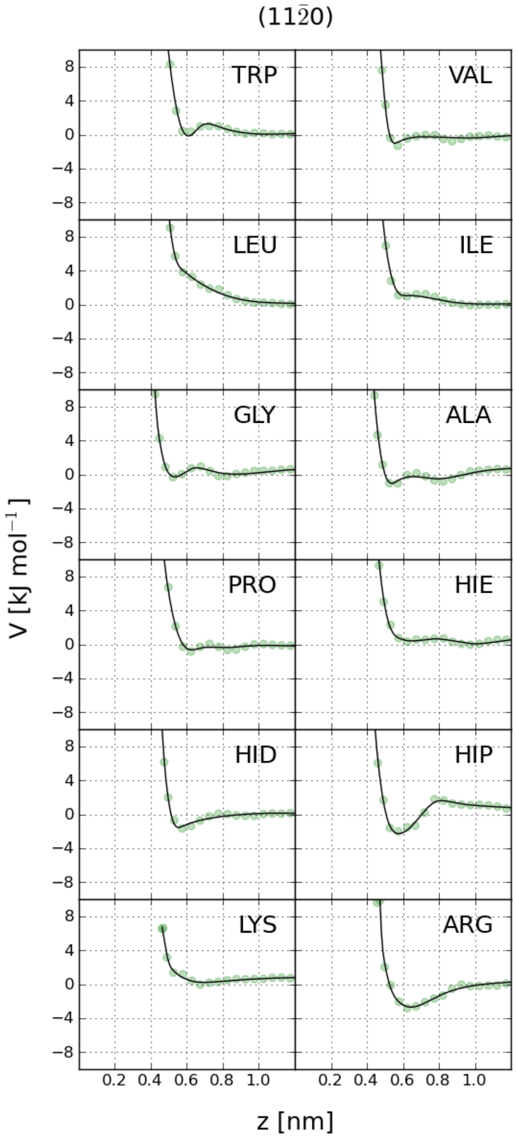

Figure 22: $V(z)$ for AAs above the (11$\bar{2}$0) surface in water – continued.

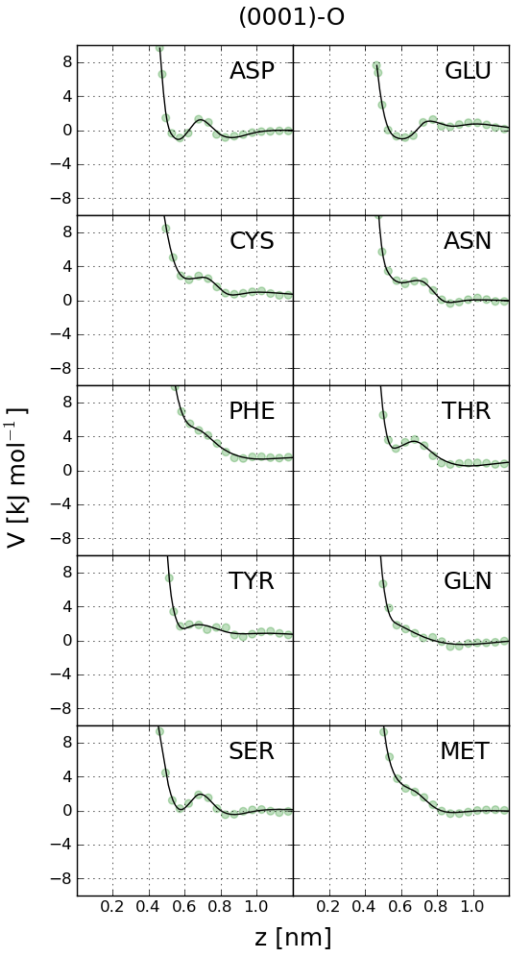

Figure 23: $V(z)$ for AAs above the (0001-O) surface in water.

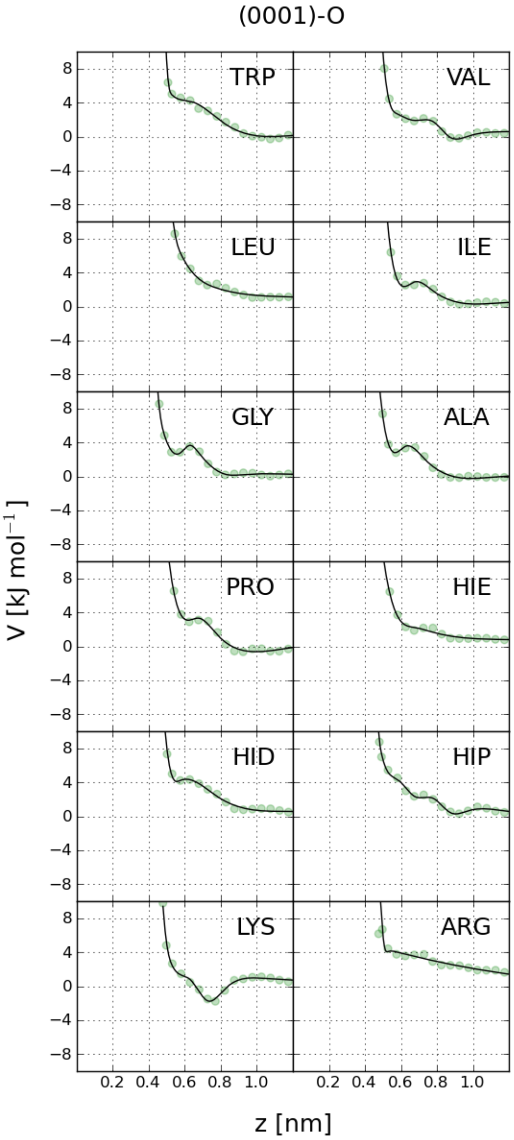

Figure 24: $V(z)$ for AAs above the (0001)-O surface in water – continued.

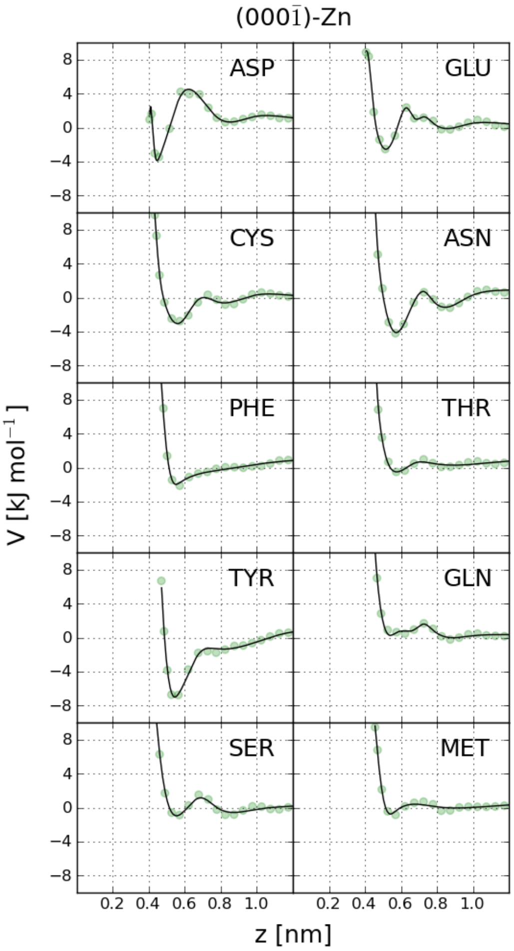

Figure 25: $V(z)$ for AAs above the (000$\bar{1}$)-Zn surface in water.

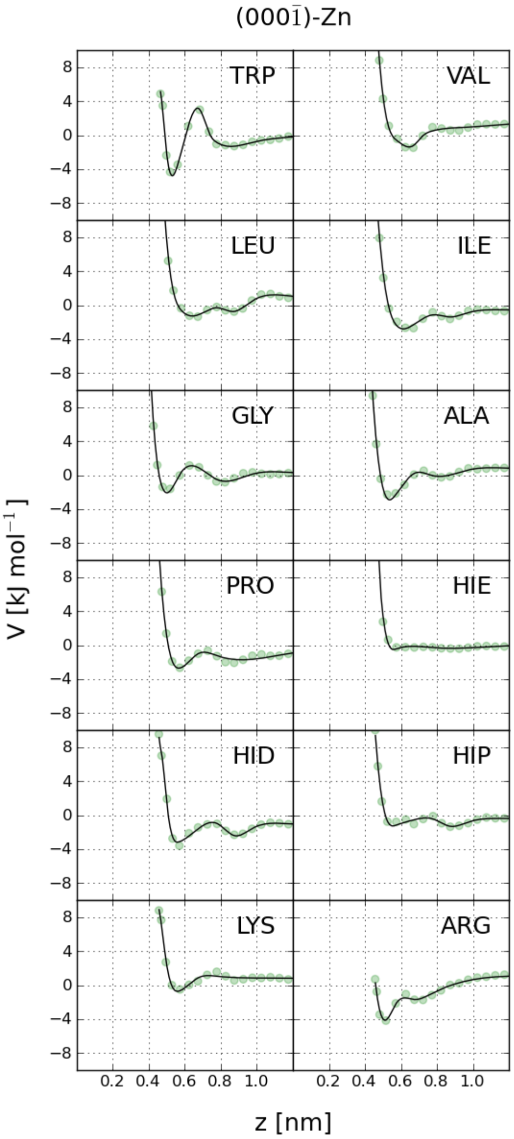

Figure 26: $V(z)$ for AAs above the (000$\bar{1}$)-Zn surface in water – continued.

Protein 1L2Y at the ZnO surfaces

The following double sets of triple panels provide an analysis of the behavior of 1L2Y during three examples of adsorption events in analogy to Figures 5 and 6 in the main text. We consider events in which at least one atom of the protein is closer than 0.5 nm to the surface for at least 1 ns.

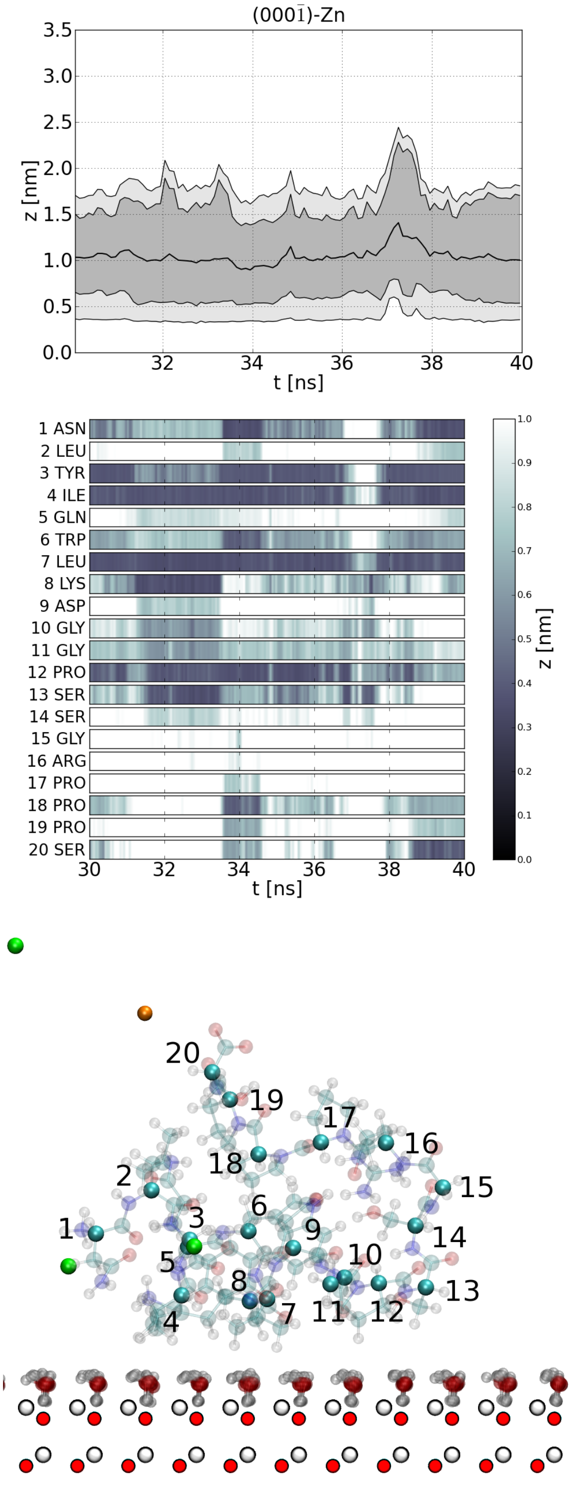

Figure 27: The behavior of the tryptophane cage near the $(000\bar{1})$-Zn surface of ZnO. The figure is an analogue of Figure 5 in the main text. In the selected time interval we identify 3 adsorption events: 31 626 - 33 376 ps, 34 876 - 36 376 ps and 38 876 - 39 876 ps. The bottom panel shown a snapshot of 1L2Y within the first event (32 000 ps).

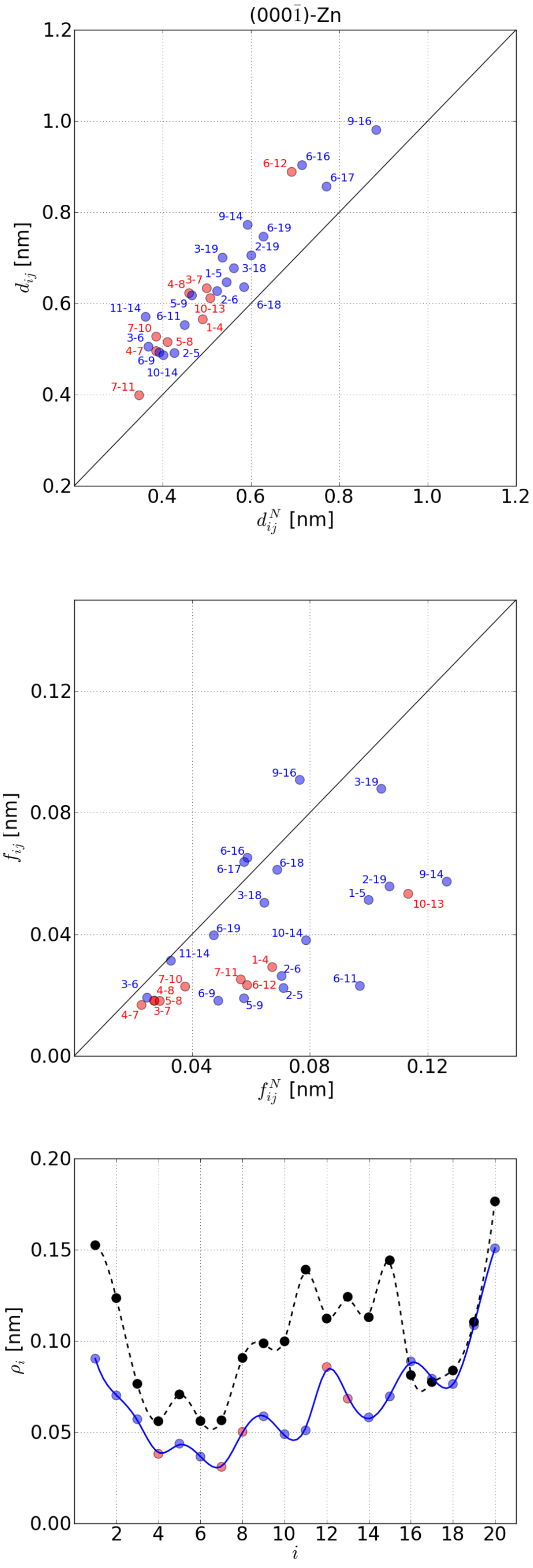

Figure 28: Fluctuational dynamics of a 1L2Y anchored to the $(000\bar{1})$-Zn surface. The lines and symbols are as in Figure 6 in the main paper. The first binding event of Figure 27 is analyzed. It involves five AAs (4, 7, 8, 12, and 13).

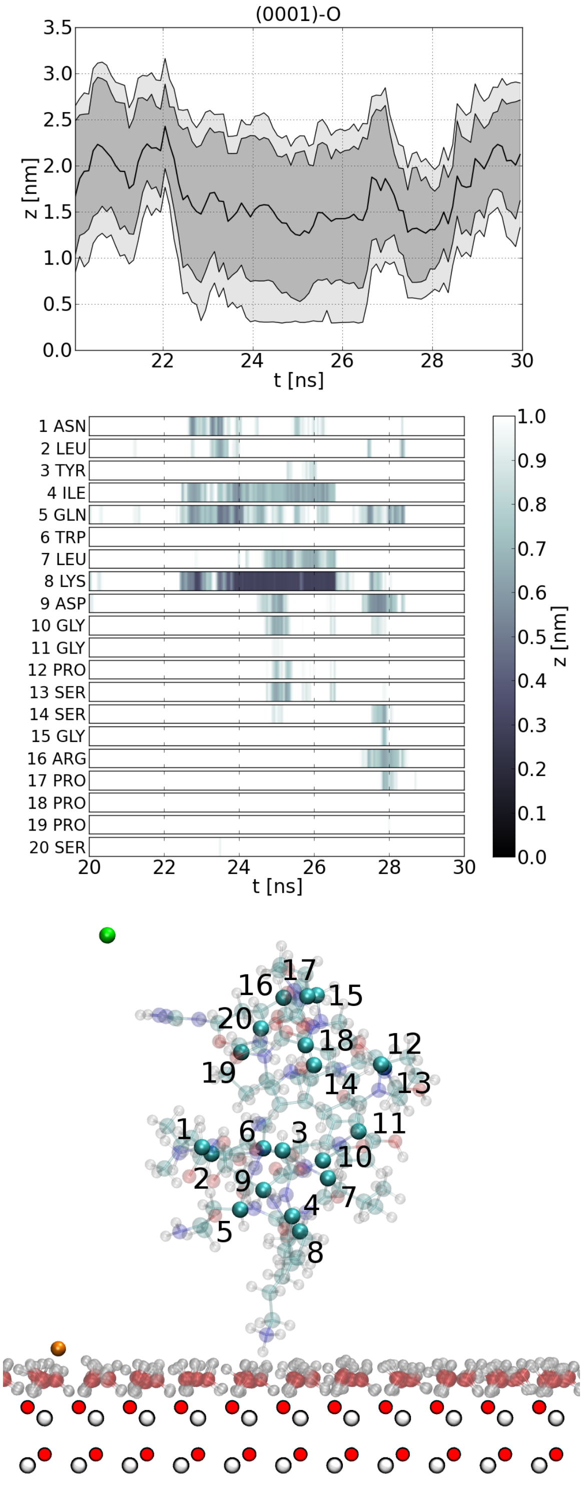

Figure 29: Similar to Figure 27 but for the (0001)-O surface. In the selected time interval we recognize adsorption event between: 23 876 and 26 376 ps. The bottom panel shows a snapshot of 1L2Y at 24 250 ps.

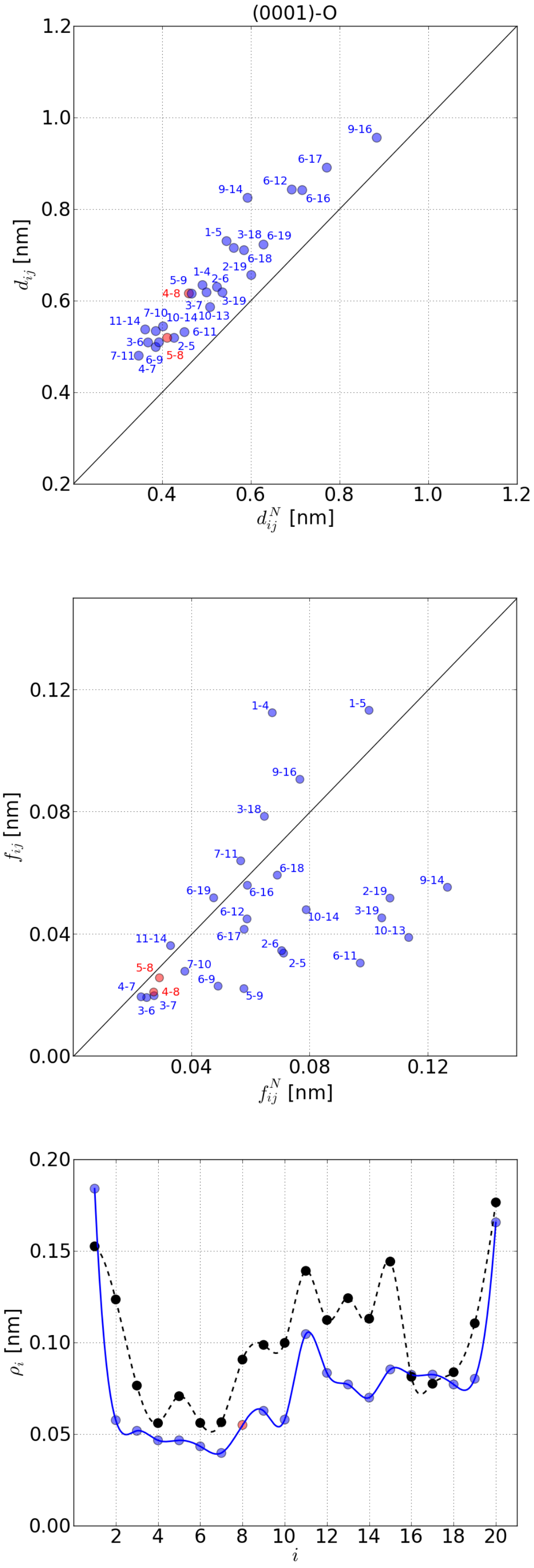

Figure 30: Similar to Figure 28. The averages are over the time interval between 23 876 and 26 376 ps of the event shown in Figure 29. It involves one AA (8)

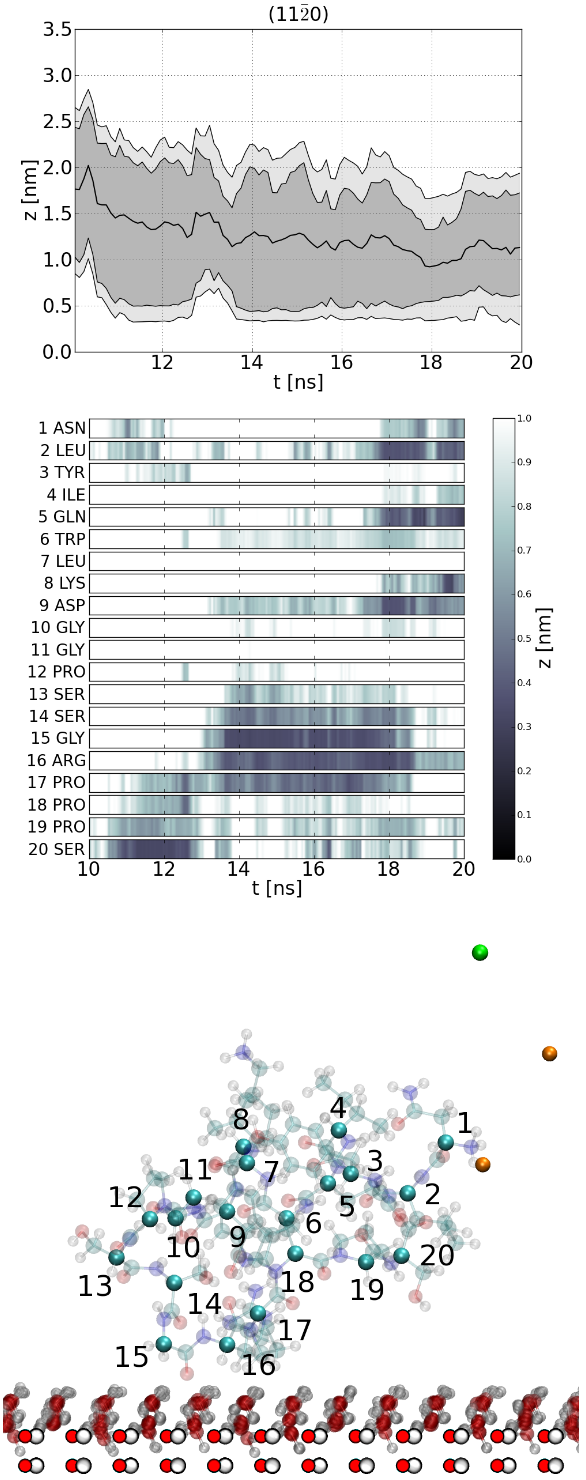

Figure 31: Similar to Figure 27 but for the (11$\bar{2}$0) surface. Between 10 876 and 12 626 only 20-SER is adsorbed. Between 15 126 and 17 126 ps the binding event involves three AAs (15, 16 and 17). The bottom panel shows a snapshot of 1L2Y at 16 000 ps.

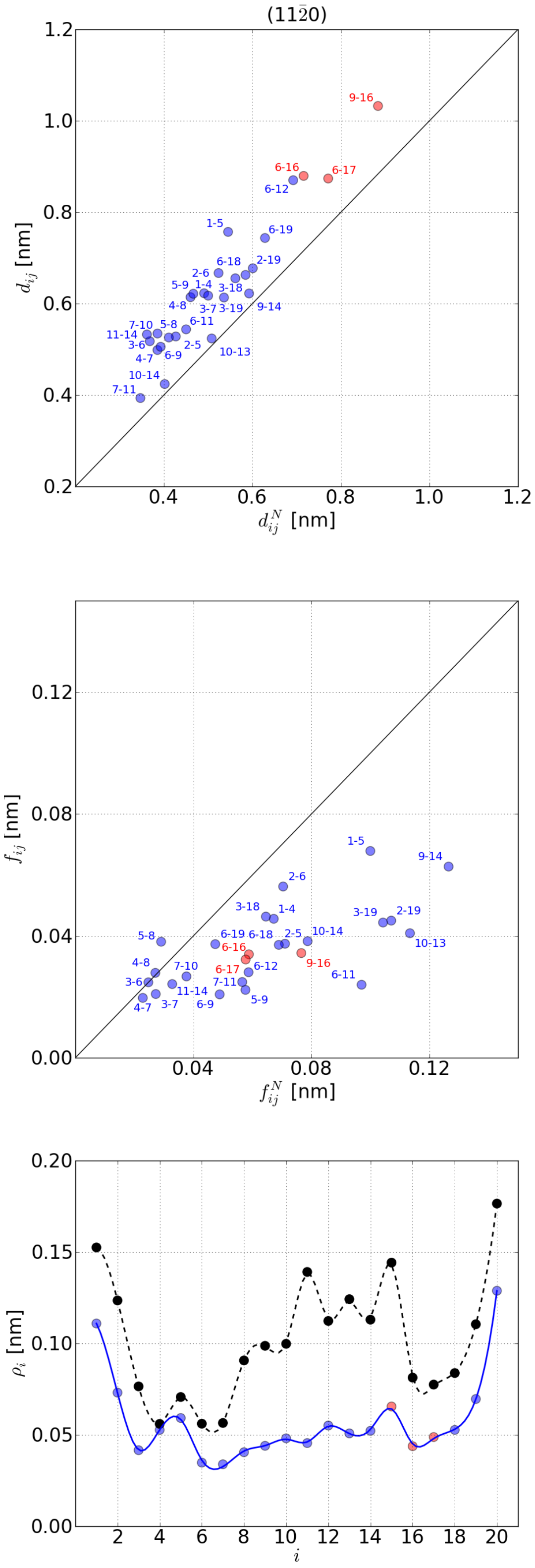

Figure 32: Similar to Figure 28. The averages are over the time interval between 15 126 and 17 126 ps corresponding to the three-AA event in Figure 31.